Modeling the antitubulin activity of benzimidazol-2-yl carbamates: Mini-review

Cite as: AIP Conference Proceedings **2388**, 030031 (2021); https://doi.org/10.1063/5.0068469
Published Online: 19 November 2021

K. L. Obydennov, O. N. Kanwugu, T. A. Kalinina, et al.

Modeling the Antitubulin Activity of Benzimidazol-2-yl carbamates: Mini-Review

K. L. Obydennov[1, a)], O. N. Kanwugu[1], T. A. Kalinina[1] and T. V. Glukhareva[1, 2]

[1]*Ural Federal University, 19 Mira Street, Ekaterinburg 620002, Russia*
[2]*Postovsky Institute of Organic Synthesis, Ural Branch of the Russian Academy of Sciences (UB RAS), 22 Sofia Kovalevskaya Street, Ekaterinburg 620990, Russia*

[a)]Corresponding author: k.l.obydennov@urfu.ru

Abstract. The biological activity of 5-benzimidazol-2-yl carbamate derivatives is associated with their ability to form a complex with *β*-tubulin and, consequently, disrupt the process of assembly of microtubules of the cytoskeleton of cells. Over the past 10 years, the understanding of the binding of 5-benzimidazol-2-yl carbamate derivatives to the *β*-tubulin subunit has increased significantly, mainly due to the published crystal structures of their ligand-receptor complexes. However, some details of this process could be predicted based on the results of molecular modeling before the publication of the corresponding crystal data. This mini-review summarizes the results of such works.

Computer modeling has become the commonly used method to explain biological activity of substances [1]. Despite the technical attractiveness of this approach, there are serious difficulties in creating a theoretical model that would correspond to the experimental data [2]. The purpose of this mini-review is to systematize scientific efforts to predict the binding site of benzimidazol-2-yl carbamate derivatives with *β*-tubulin. Interest in the generalization of these studies is due to the fact that while the crystal structure of the complex tubulin with methyl [5-(2-thienylcarbonyl)-1*H*-benzimidazol-2-yl] carbamate **1** (Fig. 1) was published only in 2015 (PDB id 5CA1), some details of the interaction of benzimidazol-2-yl carbamates with *β*-tubulin could be predicted before it. Now, as before, attempts to model the binding of benzimidazol-2-yl carbamate derivatives and *β*-tubulin are inspired by the fact that this process leads to disruption of the growth of microtubules in fungal cells [3], helminths and cancer cells. Microtubules are one of the important components of their cytoskeleton. The process of microtubule growth is based on two simultaneous processes: polymerization and depolymerization of tubulin, which lead to the so-called dynamic instability of microtubules [4]. It is known that benzimidazol-2-yl carbamate derivatives disrupt the process of tubulin polymerization and, thus, cause cell cycle arrest in the G2/M phase, leading to cell apoptosis [5]. In the course of studies of the effect of benzimidazole derivatives on tubulin polymerization in bovine brain cells [6] and in the fungus *Aspergillus nidulans* [3], it was found that 2-carbamate derivatives slow down this process, in contrast to benzimidazole itself, which showed no inhibition. In addition, competitive inhibition of tubulin polymerization was observed between benzimidazol-2-yl carbamates and colchcine **2a**, indicating similar mechanisms of their action, despite their pronounced structural differences (Fig. 1). It is known that mutations of glutamic acid 198 and phenylalanine 200 lead to resistance to benzimidazol-2-yl carbamates in both fungi [7][8][9][10][11] and helminths [12]. However, these amino acids in the *β*-tubulin molecule are located inside the protein molecule and it is not clear how the binding of benzimidazoles in this region is possible [13].

Modern Synthetic Methodologies for Creating Drugs and Functional Materials (MOSM2020)
AIP Conf. Proc. 2388, 030031-1–030031-5; https://doi.org/10.1063/5.0068469
Published by AIP Publishing. 978-0-7354-4142-2/$30.00

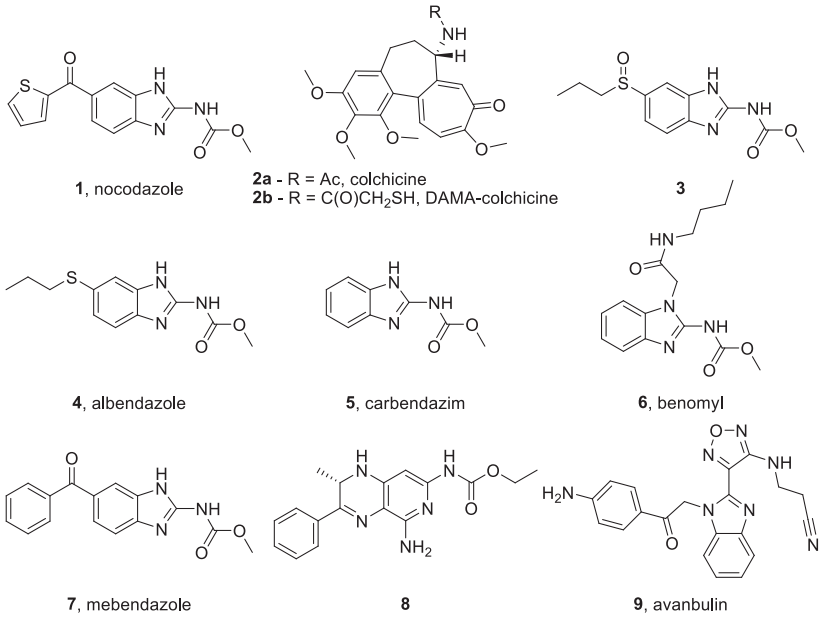

FIGURE 1. Structures of antitubulin agents

In 2004, Robinson et al. [13], in order to substantiate how deeply hidden *β*-tubulin amino acids are involved in binding to benzimidazol-2-yl carbamate derivatives, proposed an "open" form of *β*-tubulin (PDB id: 1OJ0, Fig. 2A), such a conformation in which this region of the protein would be available for interaction with benzimidazol-2-yl carbamates. This assumption was made on the basis of the following facts: the possibility of relaxation of the N-terminal (residues 1–201) and intermediate (residues 202–371) domains of tubulin relative to each other; data on the structure of the bacterial homologue of tubulin, FtsZ, in which the N-terminal domain is rotated relative to the intermediate domain by 11 °C [*]; and data that the hydrolysis of GTP by tubulin promoting depolymerization of microtubules is also associated with a rotation of the N-terminal domain by 11 °C [14].

Based on the three-dimensional structure of taxol-stabilized tubulin, in the "straight" conformation, (PDB id: 1JFF, Fig. 2A) and the amino acid sequence of tubulin of helminth *H. contortus* isotype b12-16, the authors constructed a homologous model of tubulin ("closed form") [13]. The "open" form of *β*-tubulin was obtained from the "closed" by rotating the N-terminal domain relative to the intermediate domain by 11 °C in the studied homologous model of *β*-tubulin. For this, the torsion angles of the "psi" bond between the cysteine residue Cys201 and the residue Ala382 were changed from -80.58º to -91.58º and from -65.08º to -54.08º, respectively. Methyl 6-(propylsulfinyl)-1*H*-benzo[*d*]imidazol-2-yl carbamate **3** (putative metabolite of albendazole **4**) was docked into the formed gap (Phe167 and Phe200) of the protein. The ligand-receptor complex was minimized in three stages: at a distance of 4 Å from the ligand, at a distance of 6 Å from the ligand, and at a distance of 10 Å from the ligand. After the procedure of minimization of the ligand-receptor complex, the N-terminal residue tried to return to its previous position: the torsion angle of the "psi" bond of the cysteine residue Cys201 remained -86º (in the closed form, -80.58º). The existence of an "open" form of tubulin was confirmed by crystallographic data (PDB id: 1SA0) of a "curved" conformation of tubulin in a complex with *N*-deacetyl-*N*-(2-mercaptoacetyl)colchicine (tubulin-DAMA-colchicine) **2b** [15].

Based on the docking procedure of 15 selected colchicine site inhibitors of two crystal structures of the tubulin-DAMA-colchicine complex (PDB id: 1SA0) and the tubulin-podophyllotoxin complex (PDB id: 1SA1), Tam Luong Nguyen et al. in 2005 developed a common seven-point pharmacophore model for the colchicine site [16]. Nocodazole **1** in this study was characterized by 6 pharmacophore points (A1-A2-A3-H1-H2-R1, where A1, A2, A3 - hydrogen bond acceptors; H1, H2 - hydrophobic centers; R1 - planar group). During docking, nocodazole formed two hydrogen bonds due to two C=O fragments in colchicine cavity. Nonetheless, to fit the entire pharmacophore model, nocodazole **1** lacked a fragment that would serve as a hydrogen bond donor (D). DAMA-colchicine **2b** and combrestatin A-4 (CA-4) were assigned to the A1-A2-H1-H2-R1 group. Since none of the studied compounds corresponded to all 7 points

of the pharmacophore model, this work revealed the potential for structural changes in the examined compounds, which would allow for improved binding to the colchicine site.

Subsequently, for compounds containing a trimethoxyphenyl substituent, works appeared with a successful theoretical explanation of antitubulin activity [17][18]. For example, in prior research [17], the calculated and measured free energy of binding of ligands and the receptor correlated with r2 = 0.76. However, antitubulin benzimidazol-2-yl carbamates such as nocodazole **1**, carbendazim **5**, benomyl **6**, mebendazole **7**, etc. do not contain a trimethoxyaryl fragment. Even though by 2012 12 crystal structures of ligand-receptor complexes with inhibitors of tubulin polymerization of various structures in the colchicine cavity were already described, structures with benzimidazol-2-yl carbamate derivatives have not been published. The absence of such a crystal structure caused the problem of unambiguous determination of the binding site of benzimidazol-2-yl carbamates with *β*-tubulin [19] and, consequently, the problem of quantitative analysis of structure - activity for benzimidazol-2-yl carbamate derivatives.

In 2013, RodrigoAguayo-Ortiz et al. [20] simulated the *β*-tubulin protein with the amino acid sequence of *T. spiralis* (GenBank: EFV50889) to determine the binding site of carbendazim and its 5-substituted analogs on *β*-tubulin in the MODELLER 9v10 program [21] using *β*-tubulin of *O. Aries* (PDB ID: 3N2G_D) as a template. The choice in favor of this template was made based on the fact that the complex contained ethyl [(2R)-5-amino-2-methyl-3-phenyl-1,2-dihydropyrido[3,4-b]pyrazin-7-yl] carbamate **5**, that is, a compound containing an ethyl carbamate group. Thus, it was assumed that the binding site in this protein is pre-organized for interaction with carbamate derivatives. Protein testing was carried out using PROCHECK [22] and QMEANscore [23]. It should be noted that for each benzimidazol-2-yl carbamate derivative, 4 conformers were selected, reflecting the rotation around exocyclic C-N and carbamate C-N bonds. All structures were optimized in the MMFF94x force field using Gasteiger–Marsilli atomic charges. Docking was carried out in the AutoDock 4.2 program using the Lamarkov genetic algorithm. Phe200 amino acid was chosen as the center of the docking box mesh. As a result, for each compound represented by four conformers, 1 ligand-receptor complex with the lowest free binding energy was selected. The superimposition of the obtained ligand-receptor complexes with Bos taurus tubulin heterodimer co-crystallized with DAMA-colchicine (PDB id: 1SA0) demonstrates that the binding sites of colchicinoid **2b** and both carbendazim **5** and its 5-substituted analogs are close, but do not coincide. This arrangement of binding sites explains the similar mechanism of biological action of colchicine **2a** and carbendazim **5**, which consists mainly in distortion of the T7 loop of *β*-tubulin (Fig. 2), which is thought to disrupt the interaction between heterodimers in the protofilament and lead to the process of microtubule end depolymerization.

Simulation based on docking of benzimidazol-2-yl carbamates with a homologous *β*-tubulin model constructed using *β*-tubulin of *O. Aries* (PDB ID: 3N2G) as a template explained the emergence of resistance to carbendazim and derivatives of benzimidazol-2-yl carbamates respectively in *Botrytis cinerea* [24] and helminths [25] with E198A and P198Y mutations. In particular, the importance of the amino acid Glu198 for binding to benzimidazol-2-yl carbamates has been established. The absence of hydrogen bonds with this amino acid led to a decrease in the docking score. Also, a change in phenylalanine to tyrosine at position 200 led to a weakening of these hydrogen bonds, or to their complete disappearance.

In 2014, Andrea E. Prota et al. published the first crystal structure (PDB id: 4O2A, Fig. 2A) of the complex between tubulin and 3-[(4-{1-[2-(4-aminophenyl)-2-oxoethyl]-1*H*-benzimidazol-2-yl}-1,2,5-oxadiazol-3-yl)amino] propanenitrile **9** (avanbulin) [26]. Comparison of the "curved" conformation of *β*-tubulin (PDB id: 4O2A and 4O2B) with the "straight" conformation (PDB id: 1JFF) confirmed the distortion of the T7 loop in the presence of microtubule polymerization inhibitors in the colchicine pocket (Fig. 2A). Nevertheless, the structure of BAL27862 had important differences from benzimidazol-2-yl carbamates, particularly, it did not have a carbamate group in the structure.

In 2017, PrabodhRanjan et al [27], based on the known crystal structures and the Robinson model (PDB id: 1OJ0), proposed 3 potential zones for the binding of tubulin polymerization inhibitors, located near and including the colchicine site.

In 2016, Wang et al [28] published data on the crystal structure of a complex of tubulin with nocodazole **1** (PDB id: 5CA1, Fig. 2A). It is emphasized that the complex formation does not affect the global tubulin conformation. It was shown that the main conformational changes are associated with the displacement of the T7 loop in the *β* subunit. The authors identified a new binding site in the colchicine domain: Asn165, Glu198 and Cys239. Nocodazole formed two hydrogen bonds: with glutamic acid Glu198 (Fig. 2B). The importance of Glu198 for binding to benzimidazol-2-yl carabamates is confirmed, for example, by the emergence of resistance of *Botrytis cinerea* to carbendazim **5** with the E198A mutation [29]. It is noteworthy that the amino acid at position 200 of the *β* subunit in *Gallus gallus* tubulin (PDB id: 5CA1) is tyrosine, that is, it induces resistance to benzimidazol-2-yl carbamates in fungi [30] and helminthes [12]. The location of nocadazole **1**, predicted on the basis of molecular modeling [20], differed from its location in the crystal by only an RMSD of 0.84 Å [28].

The identification of the binding site of 5-substituted benzimidazol-2-yl carbamates in 2016 has inevitably incited a number of studies into the features of this binding. In particular, the mutual influence of amino acids E198 and Y200 on their pKa was studied. It was also shown that the F200Y mutation leads to a decreases in the pKa of amino acid Glu198 from 7.38 to 6.21 [31]. Based on modeling the binding of 5-substituted benzimidazol-2-yl carbamates with different tubulin isotypes (I (βI) III (βIII) VI (βVI)) [32], a prediction was made of the possibility of re-qualification of mebendazole **7** from an anthelmintic agent (anthelmintic) to an anticancer agent [33]. Using the molecular dynamics method, the importance of a substituent at position 5 of the benzimidazole fragment for the formation of a hydrogen bond with Cys239 and imparting affinity to the molecule for binding to β-tubulin was established.

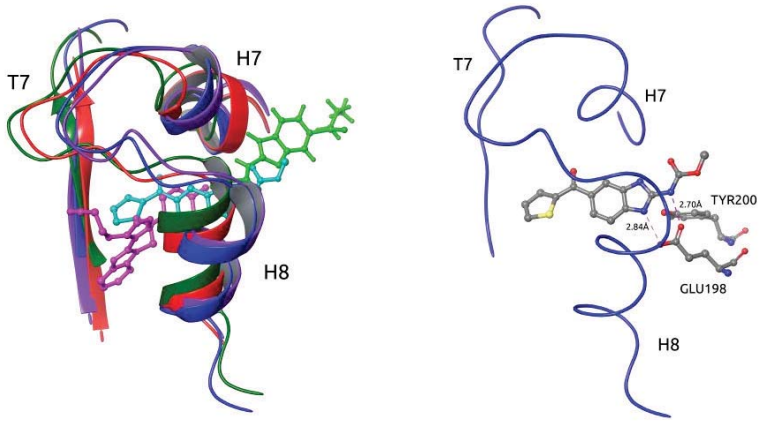

(a) (b)

FIGURE 2. (a) Overlapping of amino acid sequences 235-260 and 350-357 of β-tubulin structures (PDB id) 1JFF (red), 4O2A (purple), 5CA1 (cyan) and 1OJ0 (green). The ligand structures are shown in the following colors: avanbulin **6** - magenta color, nocodazole **1** - blue color and albendazole sulfoxide **3** - bright green color. (b) Amino acid sequence 235-260 and 350-357 from the crystal structure of the Gallus gallus T2R-TTL-Nocodazole complex (5CA1) (cyan) and the relative position of nocodazole **1** and the amino acids Glu198 and Tyr200. Made with Maestro [34].

Although data on the crystal structure of the ligand-receptor complex of nocodazole-tubulin have been published, this did not answer questions about the mechanism of action of all benzimidazol-2-yl carbamates. While the model proposed earlier [20] accurately predicted the binding to nocodazole **1**, in the case of β-tubulin binding to carbendazim **5**, it showed the weakest interaction (for docking -7.05 kcal/mol, for molecular dynamics -21.74 kJ/mol) and the absence hydrogen bond with Glu198, in contrast to the considered 5-substituted benzimidazol-2-yl carbamates. Thus, various binding sites of carbendazim **5** with β-tubulin are still considered [35][36].

For example, to substantiate the fungicidal action of carbendazim **5** against *Podosphaera xanthii*, a homologous model was proposed by [35] based on the aligned tubulin Bos taurus β-tubulin (PDB id: 1JFF) and the amino acid sequence of *P. xanthii* TUB2 gene (Genbank KC333362). The SWISS-MODEL service (www.swissdock.ch/docking) was used for blind docking of carbendazim molecules (PubChem ID: 25429) and the modeled protein. As a result, a carbendazim **5** binding site was found adjacent to the guanosine diphosphate binding site. In this case, the amino acid Thr178 formed two hydrogen bonds with the NH group of benzimidazole and the carbamate C=O group, that is, the same fragments that form the hydrogen bonds of nocodazole **1**. Additionally, the amino acid Ser138 forms a hydrogen bond with the N-atom of the benzimidazole. Also, a site (Asn204 and Ser138) adjacent to the GDP binding site for carbendazim **5** in yeast tubulin (PDB id: 5W3F) was proposed by [36]. The docking score was only -5.6 kcal / mol.

Thus, over the past 10 years, the understanding of the process of binding of 5-benzimidazol-2-yl carbamate derivatives to the β-tubulin subunit has grown significantly. Based on molecular modeling, predictions of binding of 5-substituted benzimidazol-2-yl carbamate derivatives were made, which largely describes the subsequent crystallographic data. However, there is no concession in studies to establish the binding site of carbendazim.

ACKNOWLEDGMENTS

This research was supported by the Russian Foundation for Basic Research (grant No. 18-316-20018).

REFERENCES

1. A. Sarkar and S. Sen, Int. J. Pept. Res. Ther. **26**, 209–223 (2020).
2. Y.-C. Chen, Trends Pharmacol. Sci. **36**, 78–95 (2015).
3. L. C. Davidse, J. Cell Biol. **72**, 174–193 (1977).
4. V. A. Fedorov, P. S. Orekhov, E. G. Kholina, A. A. Zhmurov, F. I. Ataullakhanov, I. B. Kovalenko, and N. B. Gudimchuk, PLOS Comput. Biol. **15**, e1007327 (2019).
5. K. Goyal, A. Sharma, R. Arya, R. Sharma, G. K. Gupta, and A. K. Sharma, Anticancer. Agents Med. Chem. **18**, 38–45 (2018).
6. P. A. Friedman and E. G. Platzer, Biochim. Biophys. Acta - Gen. Subj. **544**, 605–614 (1978).
7. Y. Zhu, X. Liang, Y. Li, Y. Duan, Z. Zheng, J. Wang, and M. Zhou, Phytopathology **108**, 352–361 (2018).
8. M. K. Jung, I. B. Wilder, and B. R. Oakley, Cell Motil. Cytoskeleton **22**, 170–174 (1992).
9. C.-J. Chen, J.-J. Yu, C.-W. Bi, Y.-N. Zhang, J.-Q. Xu, J.-X. Wang, and M.-G. Zhou, Phytopathology **99**, 1403–1411 (2009).
10. T. L. Buhr and M. B. Dickman, Appl. Environ. Microbiol. **60**, 4155–4159 (1994).
11. C. Albertini, M. Gredt, and P. Leroux, Pestic. Biochem. Physiol. **64**, 17–31 (1999).
12. R. N. Beech, P. Skuce, D. J. Bartley, R. J. Martin, R.K. Prichard, J.S. Gilleard, Parasitology **138**, 160–174 (2011).
13. M. W. Robinson, N. McFerran, A. Trudgett, L. Hoey, and I. Fairweather, J. Mol. Graph. Model. **23**, 275–284 (2004).
14. L. A. Amos and J. Löwe, Chem. Biol. **6**, R65–R69 (1999).
15. R. B. G. Ravelli, B. Gigant, P. A. Curmi, I. Jourdain, S. Lachkar, A. Sobel, and M. Knossow, Nature **428**, 198–202 (2004).
16. T. L. Nguyen, C. McGrath, A. R. Hermone, J. C. Burnett, D. W. Zaharevitz, B. W. Day, P. Wipf, E. Hamel, and R. Gussio, J. Med. Chem. **48**, 6107–6116 (2005).
17. A. Tripathi, M. Fornabaio, G. E. Kellogg, J. T. Gupton, D. A. Gewirtz, W. A. Yeudall, N. E. Vega, and S. L. Mooberry, Bioorganic Med. Chem. **16**, 2235–2242 (2008).
18. Y.-K. Chiang, C.-C. Kuo, Y.-S. Wu, C.-T. Chen, M. S. Coumar, J.-S. Wu, H.-P. Hsieh, C.-Y. Chang, H.-Y. Jseng, M.-H. Wu, J.-S. Leou, J.-S. Song, J.-Y. Chang, P.-C. Lyu, Y.-S. Chao, and S.-Y. Wu, J. Med. Chem. **52**, 4221–4233 (2009).
19. A. Massarotti, A. Coluccia, R. Silvestri, G. Sorba, and A. Brancale, ChemMedChem **7**, 33–42 (2012).
20. R. Aguayo-Ortiz, O. Méndez-Lucio, J. L. Medina-Franco, R. Castillo, L. Yépez-Mulia, F. Hernández-Luis, and A. Hernández-Campos, J. Mol. Graph. Model. **41**, 12–19 (2013).
21. A. Fiser, R. Kinh Gian Do, and A. Sali, Protein Sci. **9**, 1753–1773 (2000).
22. R. A. Laskowski, M. W. MacArthur, D. S. Moss, and J. M. Thornton, J. Appl. Crystallogr. **26**, 283–291 (1993).
23. P. Benkert, M. Künzli, and T. Schwede, Nucleic Acids Res. **37**, (2009).
24. M. Cai, D. Lin, L. Chen, Y. Bi, L. Xiao, and X. Liu, Sci. Rep. **5**, 16881 (2015).
25. R. Aguayo-Ortiz, O. Méndez-Lucio, A. Romo-Mancillas, R. Castillo, L. Yépez-Mulia, J. L. Medina-Franco, and A. Hernández-Campos, J. Mol. Graph. Model. **45**, 26–37 (2013).
26. A. E. Prota, F. Danel, F. Bachmann, K. Bargsten, R. M. Buey, J. Pohlmann, S. Reinelt, H. Lane, and M. O. Steinmetz, J. Mol. Biol. **426**, 1848–1860 (2014).
27. P. Ranjan, S. P. Kumar, V. Kari, and P. C. Jha, Comput. Biol. Chem. **68**, 78–91 (2017).
28. Y. Wang, H. Zhang, B. Gigant, Y. Yu, Y. Wu, X. Chen, Q. Lai, Z. Yang, Q. Chen, and J. Yang, FEBS J. **283**, 102–111 (2016).
29. S. Banno, F. Fukumori, A. Ichiishi, K. Okada, H. Uekusa, M. Kimura, and M. Fujimura, Phytopathology **98**, 397–404 (2008).
30. O. Yarden, Phytopathology **83**, 1478 (1993).
31. D. C. Guzmán-Ocampo, R. Aguayo-Ortiz, L. Cano-González, R. Castillo, A. Hernández-Campos, and L. Dominguez, ChemMedChem **13**, 20–24 (2018).
32. R. Aguayo-Ortiz, L. Cano-González, R. Castillo, A. Hernández-Campos, and L. Dominguez, Chem. Biol. Drug Des. **90**, 40–51 (2017).
33. A. A. Al-Karmalawy and M. Khattab, New J. Chem. **44**, 13990–13996 (2020).
34. Schrödinger (2018). Maestro. LLC, New York, USA.
35. D. Vela-Corcía, D. Romero, A. de Vicente, and A. Pérez-García, Sci. Rep. **8**, 7161 (2018).
36. R. Ahuja, A. Sidhu, A. Bala, D. Arora, and P. Sharma, Arab. J. Chem. **13**, 5832–5848 (2020).